Mechanism of fluoride removal by phosphoric acid-enhanced limestone: equilibrium and kinetics of fluoride sorption

Sweety Gogoi, Robin K. Dutta*

Department of Chemical Sciences, Tezpur University, Napaam, Tezpur 784 028, Assam, India, Tel. +919954490668; email: sgogoi4@tezu.ernet.in (S. Gogoi), Tel. +91 3712 267007/8/9, ext. 5055, +919435006674; Fax: +91 3712 267005/6; email: robind@tezu.ernet.in (R.K. Dutta)

ABSTRACT

With a fourfold increase in the selective fluoride removal capacity of limestone, to 4.38 mg/g, phosphoric acid (PA)-enhanced limestone has been found to be a competent adsorbent material for fluoride removal. The PA-enhanced limestone has been characterized and its fluoride sorption has been studied using various models. The removal of fluoride in the process has been found to take place through precipitation–adsorption. While the adsorption is monolayer in the absence of PA, intraparticle penetration of fluoride takes place in the presence of PA. Physical adsorption on hydroxyapatite and exchange between OH^- and F^- ions inside hydroxyapatite are the dominant fluoride removal mechanisms. The sorption–ion exchange is spontaneous, endothermic and follows second-order kinetics.

Keywords: Adsorption; Calcium phosphates; Hydroxyapatite; Limestone defluoridation; Phosphoric acid

1. Introduction

Fluoride is a difficult to remove inorganic contaminant of groundwater, which is causing a great problem worldwide in supply of safe drinking water. A small concentration of fluoride in drinking water is essential for human health, especially for children below 8 years of age [1]. However, excess fluoride above 1.5 mg/L in drinking water leads to serious health problems, namely, dental and skeletal fluorosis which are chronic diseases associated with mottling of teeth in mild cases and bending of bones and neurological damage in severe cases [1,2]. An excessive intake of fluoride also leads to various diseases such as arthritis, osteoporosis, brittle bones, cancer, infertility, brain damage and thyroid disorder [3].

Over 300 million people in the world are exposed to excess fluoride through drinking water. The situation is serious in India, China, Sri Lanka and the Rift Valley countries in Africa [2,4]. According to an estimate, in India alone there are about 20 million fluorosis victims and about 60 million others are exposed to the risk [4]. In Assam, a north-eastern state of India, thousands of people in Karbi Anglong, Nagaon, Golaghat, Morigaon and Guwahati metropolitan districts are severely affected by groundwater fluoride [5,6].

World Health Organization (WHO) recommends a guideline value of 1.5 mg/L for fluoride in drinking water [7]. Some developing countries have set the permissible limit of fluoride in drinking water lower than

*Corresponding author.

1.5 mg/L, because of a link between fluorosis with nutrition and total daily intake of water. For example, in India and Bangladesh the permissible limit is 1.0 mg/L [8,9]. Though alternate fluoride-free water is the best option for mitigation of the fluoride menace, piping of such water from far distances is an energy intensive, costly and time consuming affair particularly for isolated habitations. Therefore, research and development works are still on for finding a defluoridation method which is efficient and at the same time low cost, safe and simple to be used by rural people in the developing countries. Various defluoridation methods based on adsorption [10–12], electrocoagulation [13], electrodialysis [14], ion-exchange [15], precipitation [16], reverse osmosis [17], nanofiltration [18,19], etc. are known. However, each of these methods have one or more drawbacks of low efficiency, high cost, frequent replacement of parts, huge rejects, large sludge, residual toxicity, operational complicacy, etc.

Adsorption is one of the widely accepted defluoridation techniques [4]. A summary of adsorption capacities of various natural and modified adsorbent materials [20–39] are presented in Table 1. It can be seen from the table that hydroxyapatite (HAP) and brushite are the only abundant natural materials having high fluoride adsorption capacities. Though rare earth oxides have a high capacity of 12.5 mg/g [30] they are rare materials. Among the high capacity modified adsorbent materials, e.g. Al_2O_3–carbon nanotube [33], surfactant-modified pumice [36], etc. involve high-tech processes, whereas, calcined PA-treated limestone [http://www.ewisa.co.za/literature/files/148_101%20Murutu.pdf], graphene [37], tamarind fruit shell carbon [38], etc. involve energy-intensive steps like calcinations which make them less cost-effective. Moreover, materials like tamarind fruit shell may not be available in sufficient quantity [39]. In the severely fluoride affected South Asian countries, including India, HAP and brushite are not found naturally. Thus, the search for an efficient and at the same time easily available low-cost adsorbent of fluoride is still very relevant for fluoride affected regions like South Asia.

Limestone, a low-cost fluoride-adsorbing sedimentary rock is readily available in almost all fluoride affected areas in the world including India [4]. As such, limestone can adsorb fluoride to some extent.

Table 1
Comparison of monolayer adsorption capacity of limestone with some reported adsorbents

Adsorbent	Adsorption capacity (mg/g)[*]
Quartz	0.19 [20]
Red mud	0.33 [21,22]
Calcite	0.39 [20]
Magnesite	0.71 [23]
Gypsum	0.85 [23]
Laterite	0.86 [25,26]
Bauxite	1.05 [23,24]
Clays	1.69 [27,28]
Fluorspar	1.79 [20]
Hydroxyapatite (HAP)	4.54 [20]
Brushite	6.59 [29]
Rare earth oxides	12.50 [30]
Activated alumina	2.41 [29,31]
PA-enhanced limestone	4.38 [Present work]
Nano-HAP	5.50 [32]
Al_2O_3–carbon nanotube	13.5 [33]
Nano-HAP chitin composite	2.80 [34]
Bone char	2.50 [35]
Surfactant-modified pumice	41.00 [36]
Graphene	35.59 [37]
Tamarind fruit shell carbon	22.33 [38]
Carbon nanotubes	4.5 [39]
Calcined PA-treated limestone	22 [**]

*References are given within parentheses.
**http://www.ewisa.co.za/literature/files/148_101%20Murutu.pdf.

We have recently reported acid-enhanced limestone defluoridation (AELD) using a fixed bed of crushed limestone which could remove fluoride from initial 10 to 1 mg/L. In AELD, the fluoride-contaminated water is pre-acidified with edible organic acids, namely, acetic acid (AA) [40], citric acid (CA) [40] or oxalic acid (OA) [41]. The reported similar ability to remove fluoride from fluoride solution in distilled water and fluoride-containing groundwater suggested a selectivity of the method towards fluoride. The selective fluoride removal is enhanced in the presence of acid due to simultaneous fluoride removal through two mechanisms, namely, precipitation of fluoride as CaF_2 and adsorption of fluoride by limestone [40–42]. Dissolution of limestone by acid produces Ca^{2+} ions which precipitate fluoride as calcium fluoride (CaF_2). Though the neutralization of the acid by limestone is completed within a few minutes, the removal of fluoride in the AELD continues for hours [40]. This suggests that the fluoride removal continues through adsorption on the limestone surface renewed by the dissolution, even after the completion of the precipitation of CaF_2 and the calcium salt of the acid [40]. However, the fluoride removal capacities of limestone in presence of the organic acids were not competitive enough for practical applications.

Therefore, it was thought worthwhile to examine of the option of adding PA to the fluoride-containing water before treatment with limestone powder. If PA is used as the acid, the resulting calcium phosphates are also expected to adsorb fluoride like HAP which is one of the best fluoride adsorbent [43,44]. PA is acceptable in drinking water treatment [http://www. epa.gov/osw/hazard/wastetypes/wasteid/inorchem/ docs/phosphor.pdf, http://www.phosphatefacts.org/ pdf/Potable%20Water%20treatment.pdf] and also used as an additive in food and soft drinks. Our preliminary kinetics experiments have shown that the fluoride removal with PA-enhanced limestone defluoridation (PAELD) is faster than the AELD with AA, CA and OA. Moreover, the neutralization of PA by limestone is almost completed within a minute, whereas the removal of fluoride by PAELD continues for hours. The slower removal of fluoride in PAELD than the neutralization of PA by the limestone suggests that the adsorption of fluoride by the calcium phosphates significantly contributes to the total fluoride removal in the PAELD. Thus, the nature of sorption of fluoride in the PAELD is interesting from academic as well as application points of view. A systematic study of the equilibrium and the kinetics of the selective sorption of fluoride may throw light into the complex mechanism of removal of fluoride in the PAELD. Here, we report the results of a study of the equilibrium and the kinetics of the fluoride removal by limestone powder in the presence of PA, considering the fluoride removal mechanism as predominantly sorption by *in situ*-formed calcium phosphate precipitates using kinetic and equilibrium models of sorption.

2. Experimental

2.1. Materials

Powdered crude limestone samples of particle size <170 μm was obtained as a gift from Bokajan Cement Factory, Bokajan, Assam, India. The chemical composition of the limestone powder may be seen elsewhere [45]. X-ray diffraction of the sample shows the limestone to be a high quality calcite. AR grade NaF and LR grade H_3PO_4 obtained from Merck, Mumbai were used as such. Double-distilled water was used for the experiments.

2.2. Instrumental analysis

The fluoride concentrations were determined using an Orion Multiparameter Kit (Orion 4 Star pH-ISE) and a fluoride ion-selective electrode. TISAB-III was used to control ionic strength and decomplex fluoride. The pH also was determined using an Orion Multiparameter Kit (Orion 5 Star pH-ISE-Cond-DO Benchtop) using a pH electrode. The XRD data were collected on a Rigaku Miniflex X-ray diffractometer with Cu–K_α radiation ($\lambda = 0.154$ nm) at 30 kV and 15 mA using a scanning rate of 0.05°/s in 2θ and ranges from 10° to 70°. The FTIR spectra were recorded on a Nicolet Impact-410 IR spectrometer in KBr medium at room temperature in the region 4,000–500 cm^{-1}.

2.3. Methods of batch experiments

For the fluoride sorption experiments, fluoride stock solution was prepared by dissolving calculated amount of NaF in double-distilled water into which calculated volumes of 85% W/V PA was added in a 2 L volumetric flask, and then the volume was made up to 2 L. Calculated amounts of PA was added to the fluoride-containing water before mixing with limestone powder in 250 mL Erlenmeyer flasks. The mixtures were agitated in the thermostated shaker at a speed of 200 rpm at fixed temperature maintained within ± 0.5 K. For equilibrium experiments, the samples were taken out after 3 h and filtered through Whatman 42 filter paper. The remaining fluoride concentration and the pH of the filtrate were measured. The batch adsorption studies were carried out at five

different temperatures, namely, 298, 303, 308, 313 and 318 K for evaluating the thermodynamic parameters of sorption. The experiments were repeated at least thrice in order to check reproducibility.

For kinetic studies, the samples flasks were withdrawn from the shaker one by one at different times. The amounts of fluoride adsorbed by limestone in mg/g at time t (q_t) and at equilibrium (q_e) were calculated by using Eqs. (1) and (2), respectively [46]:

$$q_t = (C_0 - C_t)V/m \tag{1}$$

$$q_e = (C_0 - C_e)V/m \tag{2}$$

where C_0, C_t and C_e are the concentrations (mg/L) of fluoride initially, at time t and at equilibrium, respectively; V is the volume of the solution (L); and m is the mass of limestone taken (g).

3. Results and discussion

3.1. Fluoride removal by limestone powder in presence of PA

The effect of the dose of limestone powder on fluoride removal was studied at fixed conditions of 5 mg/L initial fluoride ($[F^-]_0$) solution (pH 1.70) and contact time of 3 h in absence and in presence of 0.10 M initial PA ($[PA]_0$). The limestone doses were varied from 0.1 to 1 g/100 mL. The fluoride removal in the presence of PA was found to be much higher than that in the absence and increased on increasing the dose of PA as shown in Fig. 1. On increasing the limestone dose in the presence of PA, the fluoride removal increased from 46% at 0.1 g/100 mL to 92% at 0.5 g/100 mL and
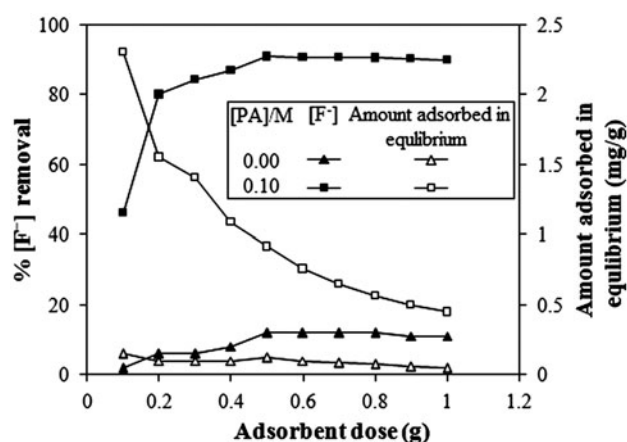
Fig. 1. Effect of limestone dose on percentage fluoride removal with the amount adsorbed in equilibrium in absence and in the presence of 0.10 M $[PA]_0$ at 298 K.

then levelled off. The levelling off may be attributed to two factors: first, overlapping of active sites occurs above a particular dose [47] and second, there cannot be any appreciable change in the effective surface area, due to conglomeration of exchanger particles at higher doses [48]. The limestone powder defluoridation in the presence of PA has been found to be much higher than that reported in presence of AA, CA and OA [40,41].

3.2. Role of sorption in the fluoride removal

The first question is whether the removal of fluoride takes place through precipitation or adsorption. CaF_2 is known to be precipitated by calcium ions generated by dissolution of limestone by acids [41]. However, the precipitation of CaF_2 is reported to be inhibited by the presence of phosphate ions [49]. On the other hand, phosphate ions of PA can combine with the calcium ions to form calcium phosphates or HAP which has a high sorption capacity of fluoride [50, http://ewisa.co.za/literature/files/148_101%20Mu rutu.pdf]. It is interesting to note that both precipitation by Ca^{2+} ions and adsorption by HAP are known to be selective towards fluoride over other ions commonly present in groundwater [41,50].

3.2.1. FTIR evidence

The FTIR spectra of fresh limestone powder show the major characteristic peaks of calcium carbonate at 1,427, 874 and 708 cm^{-1} (Fig. 2(A)) [41,51]. The peak around 3,411 cm^{-1} corresponds to the stretching frequency of O–H [52]. The spectra of the solid obtained after fluoride removal in presence of 0.10 M $[PA]_0$ also show these peaks prominently (Fig. 2(B)). The spectra of the solid obtained after use show additional peaks at 1,063 and 1,138 cm^{-1}, which can be attributed to PO_4^{3-} and H-PO_4^{2-} stretching, respectively [53]. A low intensity peak Ca–F stretching band at 749 cm^{-1} can be attributed to the presence of a small quantity of CaF_2 [54]. We have already mentioned that the precipitation of CaF_2 is inhibited by phosphate ions [49]. The IR peaks due to CaF_2 may be weak, also due to masking by the presence of very large quantity of calcium carbonate and HAP compared to that of CaF_2. Thus, IR spectra suggest that the solid, obtained after fluoride removal, contains mainly calcium carbonate [limestone] and calcium phosphate in the form of HAP along with a small quantity of CaF_2.

3.2.2. XRD evidence

The XRD patterns of the fresh limestone powder and the solid obtained after the fluoride removal in
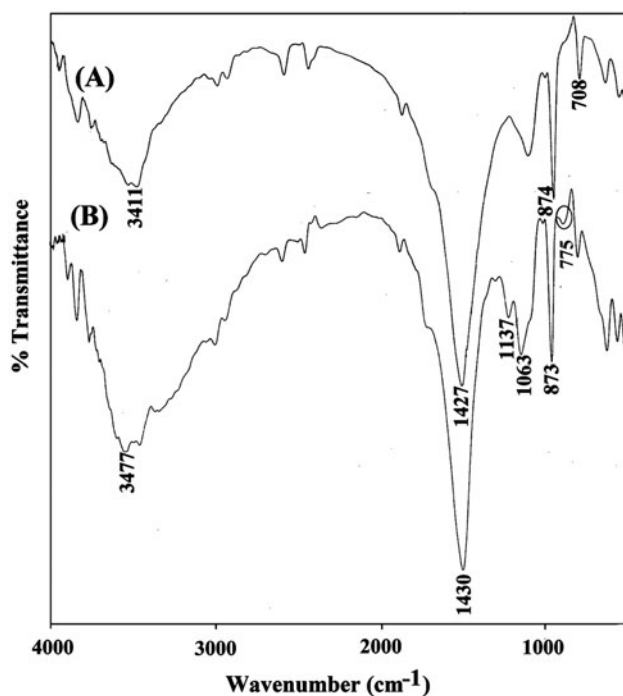
Fig. 2. FTIR spectra of limestone powder before (A) and after (B) fluoride loading.

Fig. 3. XRD of limestone powder before (a) and after (b) use for fluoride removal in presence of 0.1 M $[PA]_0$.

the presence of 0.10 $[PA]_0$ are shown in Fig. 3. The peaks with significant intensities at $2\theta = 23°$ (1 0 2), 29.5° (1 0 4) (strong), 36.12° (1 1 0), 39.5° (1 1 3), 43.5° (2 0 2), 47.5° (1 0 8) and 48.5° (1 1 6) corresponding to calcite polymorph of calcium carbonate are seen in the XRD of the fresh limestone powder. The XRD of the solid obtained after use shows all these peaks prominently, but with some changes in some relative intensities. A large increase in the relative peak intensity at 47.5° (1 0 8) in the solid obtained after fluoride removal can be attributed to diffraction from the plane (2 0 2) of fluorite (CaF_2) [55]. An absence of any significant quantity of fluorite [CaF_2] in the solid obtained after fluoride removal is indicated by the absence of a significant peak of fluorite expected at 46.9° (2 2 0) [56,57]. Variations in the relative intensities of the peaks were reported also with limestone after use in AELD with AA, CA and OA [40,41], which were attributed to adsorption of fluoride on the limestone surfaces. Thus, it is possible that the evidences of the presence of fluorite in the solid obtained after fluoride removal is due to fluoride adsorbed on limestone rather than precipitated fluorite.

The large increase in the relative peak intensity observed at 47.5° (1 0 8) after fluoride loading may also be attributed to contribution by (1 0 8) plane of HAP [52]. The peaks at 56.20° (3 2 2), 50.86° (2 3 1),

40.80° (3 1 0) and 32.10° (2 2 2) also correspond to HAP [52]. This indicates that a significant formation of HAP takes place in the process. Small peaks at 31.92° (2 1 1) and 42.7° (1 3 1) correspond to fluorapatite (FAP) [52]. The FAP may have formed due to adsorption of fluoride by HAP, since HAP has a very strong affinity for adsorption of fluoride [32,44]. Thus, the above evidences suggest that the fluoride removal in the present process is dominated by adsorption by two adsorbents. The major adsorbent is HAP which forms FAP after sorption of fluoride through ion exchange and the minor adsorbent is the limestone itself. The mechanism will be clear from the subsequent studies on adsorption equilibrium and kinetics.

3.2.3. Kinetics of neutralization of PA by limestone powder

The initial pH of 0.10 M PA was 1.70, which finally increased to above 6.00 after neutralization by limestone. The equilibrium pH of treated water was found to be in the range 6.00–6.50. However, remaining pH of the treated water can be increased to pH 7 by treatment of the effluent with another crushed limestone reactor [58]. The kinetics of neutralization of PA by limestone powder and the kinetics of removal of fluoride by PAELD have been compared in Fig. 4. It has been seen that the acid is almost neutralized within a
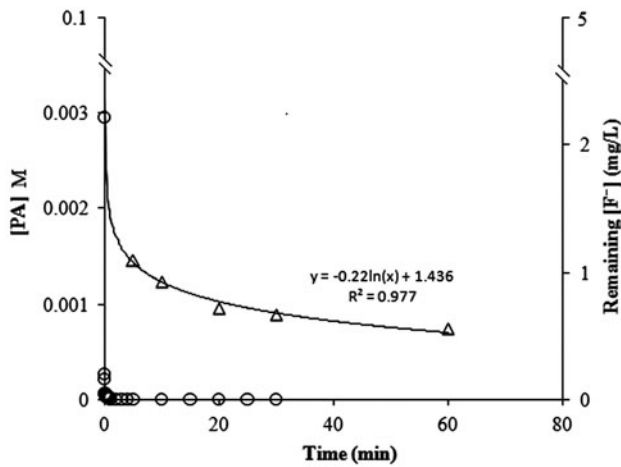
Fig. 4. A plot of neutralization of PA and remaining [F⁻] vs. time in PAELD.

minute, whereas the fluoride removal, though faster initially, continues for hours. Therefore, the dissolution of limestone by PA and the precipitation of calcium phosphates is a rapid process and it is quite possible that the dominant mechanism of fluoride removal is a slower adsorption or sorption by the co-produced calcium phosphates. However, the validity of this assumption and the role and nature of sorption will be clear from the results of the following experiments.

3.2.4. Effect of contact time on fluoride removal

The removal of fluoride as a function of contact time for different $[PA]_0$ and $[F^-]_0$ are shown in Fig. 5(A) and (B), respectively. The figures show that the removal of fluoride continued to increase on increasing contact time up to 50 min and the equilibrium is reached within 3 h. The same trend was observed with other $[PA]_0$ and $[F^-]_0$. Thus, the fluoride removal increases with increase in $[PA]_0$, but decreases with increase in $[F^-]_0$ (Fig. 5(B)) as was reported with other acids [41].

3.3. Adsorption kinetics

The kinetics of adsorption of fluoride has been investigated through pseudo-first-order, pseudo-second-order, intraparticle diffusion and Elovich kinetic models. The pseudo-first-order and the pseudo-second-order equations can be expressed by Eqs. (3) and (4), respectively [59,60]:

$$\ln(q_e - q_t) = \ln q_e - k_1 t \tag{3}$$
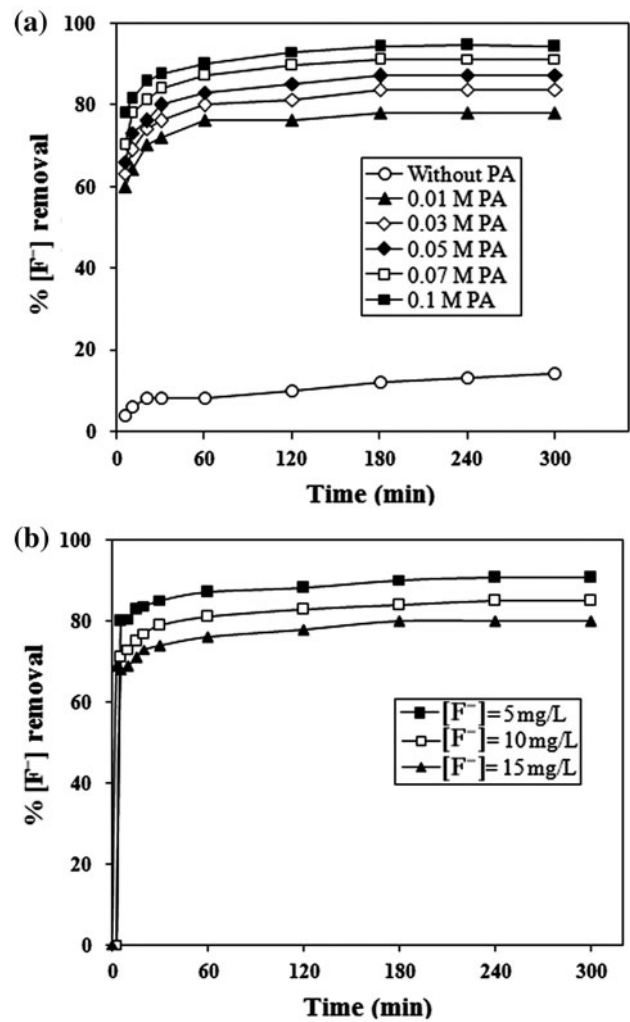
Fig. 5. Effect of contact time on fluoride removal by limestone powder in presence of varying $[PA]_0$ (a) and $[F^-]_0$ (b) at 298 K.

$$t/q_t = (1/k_2)(1/q_e^2) + (t/q_e) \tag{4}$$

where q_e (mg/g) and q_t (mg/g) are the amount of fluoride adsorbed at equilibrium and at time t (min), respectively. k_1 (1/min) and k_2 (g/mg min) are the pseudo-first-order and the pseudo-second-order rate constants. The values of q_e and k_1 have been determined from the slope and the intercept of the linear plot of $\ln(q_e - q_t)$ against t. k_2 and adsorption affinity $(k_2 q_e^2)$ have been evaluated from the slope and the intercept of the linear plot of t/q_t vs. t. The plots are shown in Fig. 6.

The correlation coefficient values (Table 2) obtained from the linear pseudo-first-order plot (Fig. 6(A)) are poor (<0.952) and the adsorption capacity (q_e, cal) calculated from the plot does not match
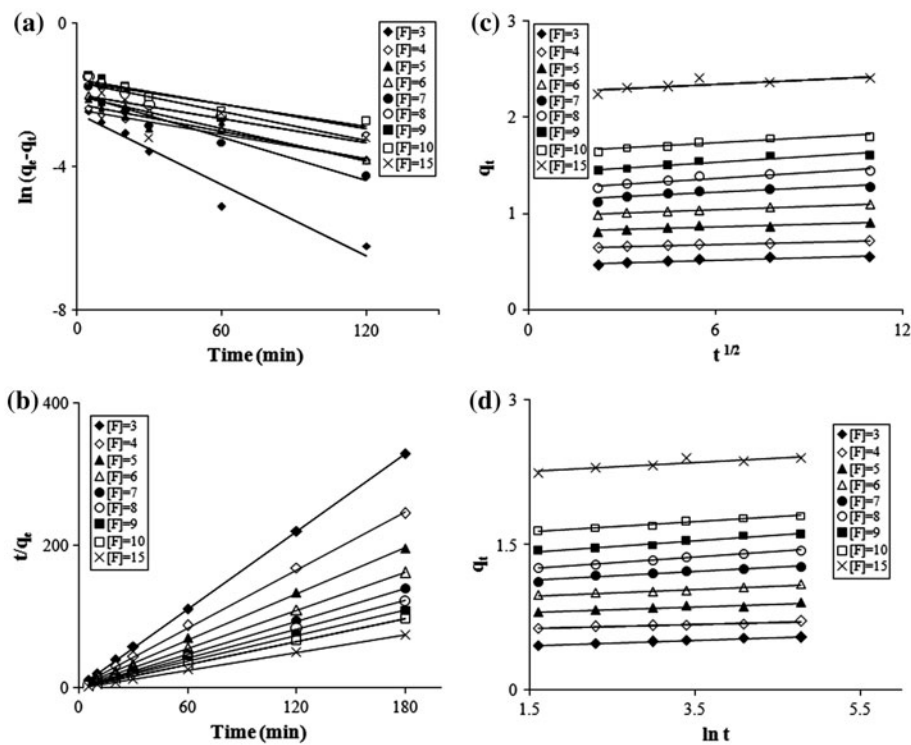
Fig. 6. Plots of pseudo-first-order (a), pseudo-second-order (b), intraparticle diffusion (c) and Elovich (d) kinetic models of fluoride adsorption by in limestone–PA system at different $[F^-]_0$ with fixed $[PA]_0$ (0.10 M) and adsorbent dose (0.5 g/100 mL) at 298 K.

Table 2
Adsorption parameters obtained from pseudo-first-order, pseudo-second-order, intraparticle diffusion and Elovich models for adsorption of fluoride by limestone powder in the presence of PA with varying $[F^-]_0$, $[PA]_0 = 0.10$ M and adsorbent dose = 0.5 g/100 mL at 298 K

	$[F^-]_0$ (mg/L)								
Parameter	3	4	5	6	7	8	9	10	15
Pseudo-first-order model									
k_1	0.033	0.014	0.012	0.014	0.020	0.013	0.011	0.010	0.007
q_e,(cal)	0.081	0.094	0.104	0.133	0.137	0.194	0.208	0.168	0.197
q_e,(exp)	0.548	0.736	0.924	1.114	1.292	1.482	1.675	1.864	2.446
R^2	0.952	0.948	0.878	0.945	0.947	0.929	0.830	0.893	0.904
Pseudo-second-order model									
k_2	1.225	0.737	0.617	0.562	0.473	0.567	0.326	0.295	0.435
q_e,(cal)	0.552	0.737	0.925	1.118	1.298	1.485	1.672	1.865	2.444
q_e,(exp)	0.548	0.736	0.924	1.114	1.292	1.482	1.675	1.864	2.446
R^2	1.000	0.999	0.999	0.999	0.999	0.999	0.999	0.999	0.999
Intraparticle diffusion model									
k_i	0.009	0.007	0.009	0.012	0.016	0.020	0.020	0.018	0.015
R^2	0.862	0.974	0.845	0.982	0.834	0.904	0.896	0.915	0.656
Elovich model									
A	1.54×10^5	5.50×10^{11}	5.63×10^{10}	1.93×10^{10}	1.79×10^8	3.28×10^7	3.95×10^8	5.15×10^{12}	2.63×10^{18}
$1/B$	0.027	0.020	0.027	0.034	0.048	0.058	0.059	0.052	0.048
R^2	0.970	0.963	0.913	0.979	0.960	0.988	0.957	0.981	0.798

well with experimental values, which indicate a poor fitting of pseudo-first-order model in the process. But as reported earlier, the large k_1 values indicate the feasibility of a pseudo-first-order model [60].

In case of the pseudo-second-order plot (Fig. 6(B)), the correlation coefficient values are found to be in the range between 1.000 and 0.999, which is much better than that of pseudo-first-order plots (Table 2). The calculated equilibrium capacities (q_e, cal) also match well to those obtained from experiment. Both the pseudo-first-order rate constant (k_1) and the pseudo-second-order rate constant (k_2) decreased with increase in of $[F^-]_0$ which may be due to decrease in the solid–solute ratio on increasing the $[F^-]_0$.

The intraparticle diffusion model has been used to evaluate the rate-determining step, as well as whether the sorption takes place at outer surface or in the internal pores and voids within the matrix of the adsorbent [60]. Kadirvelu et al. [61] model has been used to describe intraparticle diffusion where the amount of fluoride adsorbed by limestone in mg/g at time t, q_t is expressed by Eq. (5):

$$q_t = k_i t^1/2 \tag{5}$$

where k_i (mg/g min$^{1/2}$) is the intraparticle diffusion rate constant. The values of k_i can be evaluated from the plot of q_t vs. $t^{1/2}$ (Fig. 6(C)). The intraparticle diffusion rate constant (k_i) for various $[F^-]_0$ were determined from the slope of respective plots (Table 2). The observed linearity of the curves indicates the occurrence of intraparticle diffusion. However, the intraparticle diffusion may not be the only rate-controlling step because the plots did not pass through the origin. Perhaps, the precipitation of calcium salts also complicates the process. Since the values of k_i increases with increase in $[F^-]_0$, the i1ntraparticle diffusion may be considered as concentration-dependent diffusion [62].

The Elovich rate equation is used for describing kinetics of chemisorptions [63]. The simplified form of this model is represented by Eq. (6)

$$q_t = (1/B) \ln AB + (1/B) \ln t \tag{6}$$

where A (mg/g min^{-1}) is the sorption constant of the fluoride ions and B (g/mg) is the desorption constant of the fluoride ions. The slope of the plots of q_t vs. $\ln t$ (Fig. 6(D)) gives the values of $1/B$. The desorption constant ($1/B$) values ranged from 0.027 to 0.059 mg/g at different $[F^-]_0$, which suggests that the number of available active sites to sorb fluoride decreases with increase in $[F^-]_0$ (Table 2). The correlation coefficient

values lie between 0.913 and 0.988 (except with highest $[F^-]_0$) indicating suitability of this model. From the correlation coefficient values, the order of the appropriateness of the kinetic models for adsorption of fluoride on limestone in presence of PA has been found to be: pseudo-second-order > pseudo-first-order > Elovich > intraparticle diffusion.

3.4. Adsorption isotherms

The equilibrium adsorption data with $[F^-]_0$ in the range of 3–15 mg/L were fitted to linearly transformed Freundlich and Langmuir equations (Fig. 7(A) and (B)). The linear forms of Freundlich isotherm can be represented by Eq. (7) [64]:

$$\ln q_e = \ln K_F + 1/n \ln C_e \tag{7}$$

where q_e, C_e, K_F and n are the amount of fluoride adsorbed at equilibrium (mg/g), the fluoride concentration at equilibrium (mg/L), the Freundlich adsorption capacity (mg/g) and adsorption intensity, respectively. The values of K_F and n were determined from the intercept and slope of the linear plot of $\ln q_e$ vs. $\ln C_e$ (Fig. 7(A)) (Table 3). Values of $1/n$ were between 0.10 and 1.0 and the n values were between 1 and 10 which confirm the existence of favourable conditions for adsorption [64]. In the absence of PA, limestone showed a poor adsorption capacity of ≈0.37 (mg/g) similar to the earlier reported values [20] with a squired correlation coefficient (R^2) of 0.951. The correlation coefficients values were good (≈0.974), but the adsorption capacity values were low in the presence of 0.01 M PA. The correlation coefficients values, however, gradually decreased to 0.834 on increasing the concentration of PA up to 0.10 M. The adsorption capacity (q_e) increased with increase in $[PA]_0$ which may be due to two factors: first, due to increase in adsorption on renewed limestone surface due to dissolution of limestone by the acid [40,41] and second, due to adsorption of fluoride by newly formed calcium phosphates like HAP, through reaction between limestone and PA [50, http://www.ewisa.co.za/litera ture/files/148_101%20Murutu.pdf].

The Langmuir isotherm can be expressed by Eq. (8) [64]:

$$C_e/q_e = C_e/Q_o + 1/bQ_o \tag{8}$$

where Q_o and b are the adsorption capacity (mg/g) based on Langmuir isotherm and the Langmuir isotherm constant (L/mg) related to the affinity of the
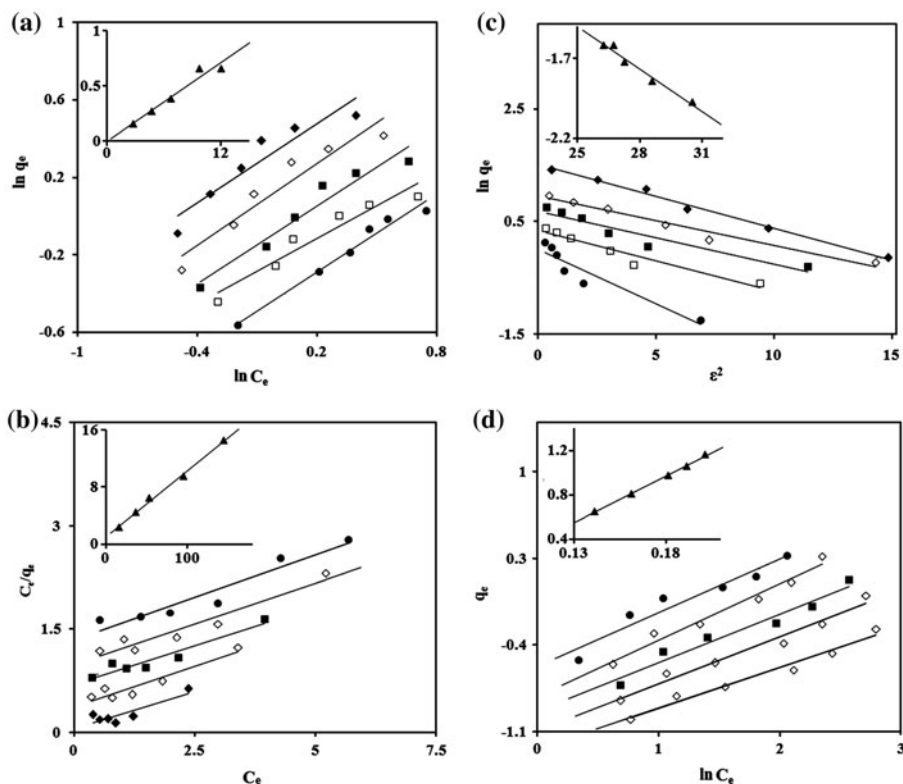
Fig. 7. Freundlich (a), Langmuir (b), Dubinin–Radushkevich (c) and Temkin (d) isotherms for fluoride adsorption on limestone powder at fixed adsorbent dose (0.5 g/100 mL) and contact time (3 h) at 298 K. $[F^-]_0$: 3–15 mg/L^{-1}, $[PA]_0$: 0.01 M (●) 0.03 M (□), 0.05 M (■), 0.07 M (◊), 0.10 M (♦) and 0.00 M (inset, ▲).

binding sites, respectively. The Q_o and b values were calculated from slope and intercept of the plot of C_e/q_e vs. C_e (Fig. 7(B)). The calculated values are included in Table 3. The R^2 values in presence of PA decreased on increasing [PA] in a similar way as was observed with the Freundlich model.

The maximum fluoride adsorption capacities of limestone powder in absence and in the presence of PA have been found to be 1.10 and 4.38 mg/g, respectively. It is interesting to note a fourfold higher fluoride removal capacity of PA-enhanced limestone powder compared to the crude limestone powder. The PA-enhanced limestone which shows comparable fluoride adsorption capacity with HAP and brushite (Table 1), can be of great potential for application in the severely fluoride-affected regions like South Asia where limestone is readily available, but HAP and brushite do not occur naturally. The PA-enhanced limestone is advantageous over other modified adsorbent materials such as Al_2O_3–carbon nanotube [33], surfactant-modified pumice [36], tamarind fruit shell carbon [38], calcined PA-treated limestone [http://www.ewisa.co.za/literature/files/148_101%20Murutu.pdf], graphene [37], etc. (Table 1) as the present process does not involve any

sophisticated or energy-intensive techniques and can be used without electricity. In addition, there are scopes for further improvement of the capacity of PA-enhanced limestone through application of nanotechnology and process optimization.

The results suggest that the adsorption behaviour of fluoride on limestone in the presence of PA does not fit well to either of the Freundlich and the Langmuir models. However, the Freundlich model fits somewhat better than the Langmuir model. This behaviour can be explained by considering the fluoride removal by both physical adsorption on limestone or HAP and ion exchange between F^- and CO_3^{2-} ions inside limestone particle or between F^- and OH^- ions inside HAP as shown in the following equations [20,34]:

$$2F^- + CaCO_3(s) = CaF_2(s) + CO_3^{2-} \qquad (9)$$

$$F^- + Ca_5(PO_4)_3OH(s) = Ca_5(PO_4)_3F(s) + OH^- \qquad (10)$$
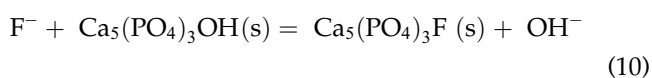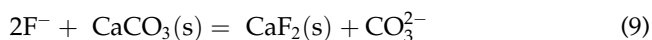
Such fluoride removal by combination of adsorption and ion-exchange mechanisms are reported in fluoride

Table 3
Values of Freundlich, Langmuir, Dubinin–Radushkevich and Temkin isotherm parameters for fluoride adsorption on limestone in absence and presence of $[PA]_0$ at 298 K

Isotherm model	$[PA]_0$/(M)					
	0.00	0.01	0.03	0.05	0.07	0.10
Freundlich						
K_F	0.988	0.997	1.020	1.208	1.489	1.932
n	1.497	1.044	1.550	1.531	1.490	1.307
R^2	0.951	0.974	0.932	0.942	0.917	0.834
Langmuir						
Q_0	1.104	4.032	3.400	3.802	4.000	4.380
b	0.093	0.155	0.483	0.493	0.636	0.748
R^2	0.996	0.924	0.927	0.920	0.891	0.768
Dubinin–Radushkevich						
B_D	0.088	0.284	0.162	0.120	0.112	0.112
Q_D	2.691	1.702	2.029	2.088	2.442	2.992
E	6.743	1.327	1.756	2.041	2.113	2.113
R^2	0.971	0.889	0.937	0.903	0.968	0.989
Temkin						
A_T	0.860	0.740	0.452	0.439	0.392	0.485
B_T	8.441	0.468	0.548	0.512	0.479	0.391
R^2	0.998	0.927	0.971	0.955	0.970	0.957

removal by HAP and n-HAP [20,34]. It can be seen from Table 3 that the adsorption coefficient, b, which is related to the apparent energy of adsorption, is increased from 0.155 to 0.748 L/mg on increasing [PA] from 0.01 to 0.10 M. The increase in b with [PA] may be attributed to increased quantity of the actual major adsorbent produced *in situ*, i.e. HAP. The plots of the concentrations of calcium and phosphate as phosphorous remaining in the treated water as a function of $[PA]_0$ are shown in Fig. 8. The deviations in the curves of the plots of the concentrations of calcium and phosphate as phosphorous vs. $[PA]_0$ from linearity suggest increased precipitation of calcium phosphate at higher $[PA]_0$.

The feasibility of the Langmuir isotherm is expressed in terms of dimensionless equilibrium parameter, R_L, defined by the following equation [65]:

$$R_L = 1/(1 + bC_0) \qquad (11)$$

where C_0 is the $[F^-]_0$. The R_L values (Table 4) are smaller than 1 at the experimental $[F^-]_0$ and $[PA]_0$ and decrease with increase in the initial concentrations of both. This indicates that the adsorption is favourable and increases with the concentrations of both fluoride and PA.

Dubinin–Radushkevich (D–R) isotherm equation [66] helps in understanding whether the adsorption is
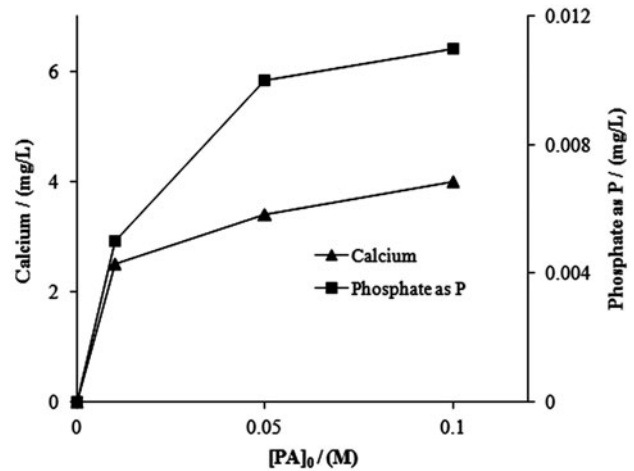
Fig. 8. Plots of the concentrations of calcium and phosphate as phosphorous remaining in the treated water vs. $[PA]_0$.

Table 4
The values of R_L obtained from the Langmuir constant, b at different $[F^-]_0$ and $[PA]_0$ at 298 K

$[F^-]_0$ (mg/L)	$[PA]_0$/(M)				
	0.01	0.03	0.05	0.07	0.10
3	0.683	0.408	0.043	0.344	0.308
5	0.563	0.293	0.287	0.239	0.211
7	0.479	0.229	0.225	0.183	0.160
10	0.392	0.172	0.168	0.136	0.118
15	0.301	0.121	0.119	0.095	0.081

physisorption or chemisorption. The low E values observed in the present case indicate physisorption of fluoride [66]. This equation is expressed in the linear form as:

$$\ln q_e = \ln Q_D - B_D \varepsilon^2 \qquad (12)$$

where Q_D is the adsorption capacity (mg/g), B_D is the activity constant related to mean sorption energy (mol^2/kJ^2) and ε is the Polanyi potential which is defined by Eq. (13):

$$\varepsilon = RT \ln(1 + 1/C_e) \qquad (13)$$

where R is the gas constant (J/Kmol) and T is the temperature in K. The mean free energy of adsorption, E (kJ/mol), can be calculated from B_D using Eq. (14).

$$E = 2B_D^{-0.5} \qquad (14)$$

The plot of $\ln q_e$ vs. ε^2 is shown in Fig. 7(C) and the values of the constants Q_D and B_D calculated from the slope and the intercept, respectively, are included in Table 3. The reasonably good R^2 values indicate that the adsorption of fluoride by limestone powder in presence of PA fits well to the D–R model. The fitting improved with increase in $[PA]_0$. The calculated E values have been found to be in the range between 1 and 6 kJ/mol (Table 3), which suggest that the adsorption of fluoride on limestone in presence or absence of PA takes place through physisorption.

The Temkin isotherm equation can be represented by the following equation [67]:

$$q_e = B_T \ln A_T + B_T \ln C_e \qquad (15)$$

A_T (L/g) is the binding constant that represents the maximum binding energy and $B_T = (RT)/b$ is the Temkin constant related to heat of sorption. The plot of q_e vs. $\ln C_e$ generates a straight line (Fig. 7(D)). The values of A_T and B_T are calculated from the slope and the intercept, respectively (Table 3). The R^2 values indicate that the present system fits well to the Temkin model. The B_T values in the presence of PA are considerably lower than that in the absence of PA. Temkin isotherm equation assumes that the heat of adsorption decreases linearly with coverage due to adsorbate–adsorbate interactions and that the adsorption is characterized by a uniform distribution of the binding energies, up to some maximum binding energy [67]. The enthalpy of ion exchange can be as low as the enthalpy of physisorption [68]. The observed lower values in B_T in the presence of PA may indicate a lower heat of exchange of OH⁻ ions of HAP by F⁻ ions than the adsorption of F⁻ ions on limestone. It may be noted here that fluoride ions replace OH⁻ ions of HAP to form FAP in the present case. Therefore, in the present case, B_T is probably a function of the enthalpy of exchange of OH⁻ ions by F⁻ ions rather than simple adsorption of the latter. Based on the R^2 values, the suitability of the adsorption isotherms follow the order: Temkin > Freundlich > D–R > Langmuir. Thus, it appears from the adsorption isotherms that the removal of fluoride in the PA-enhanced limestone takes place through exchange of OH⁻ ions of HAP by F⁻ ions which is energetically comparable to physisorption [68].

3.5. The thermodynamics of adsorption

The thermodynamic parameters such as standard free energy change ($\Delta G°$), enthalpy change ($\Delta H°$) and entropy change ($\Delta S°$) of adsorption were calculated using the following equations [69]:

$$(\Delta G°) = -RT \ln K_c \qquad (16)$$

$$\ln K_c = \Delta S°/R - \Delta H°/RT \qquad (17)$$

where K_c is the standard equilibrium constant of adsorption. A plot of $\ln K_c$ vs. $1/T$ for 5 mg/L $[F^-]_0$ in presence or absence of PA gives a straight line and the values of $\Delta H°$ and $\Delta S°$ have been estimated from the slope and the intercept, respectively (Fig. 9). The values of thermodynamic parameters are listed in Table 5.

The negative value of $\Delta G°$ at all temperatures in presence of PA implies that the reaction is spontaneous. The free energy becomes more negative with increase in $[PA]_0$ and the temperature. The free energy of adsorption is low, but sufficiently high to provide a favourable equilibrium fluoride adsorption, as has been observed. However, the values of $\Delta G°$ are positive at all temperatures for the adsorption of fluoride on limestone in absence of PA, which confirms that adsorption of fluoride on limestone powder, is very weak. The positive values of $\Delta H°$ suggest that the adsorption of fluoride on limestone in all cases is endothermic in nature [69]. Li et al. attributed similar increase in adsorption with temperature to positive $\Delta H°$ [37]. The positive $\Delta S°$ actually makes the $\Delta G°$ more and more negative on increasing temperature which causes the adsorption to increase with increase in the temperature. The entropy change is positive and increases with increase in the $[PA]_0$. This indicates
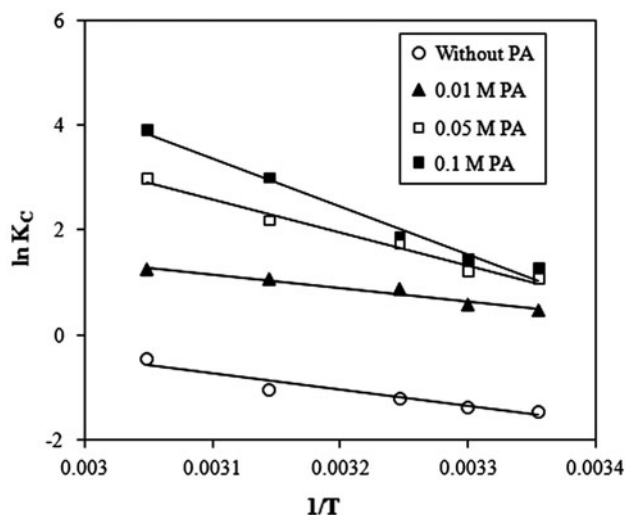
Fig. 9. Plots of $\ln K_c$ vs. $1/T$ for the adsorption of fluoride by limestone powder from aqueous solution in the presence or absence of $[PA]_0$.

Table 5
Thermodynamic parameters for the adsorption of fluoride on limestone in absence or presence of PA at different $[PA]_0$. The $\Delta S°$ and $\Delta H°$ values are at 298 K

$[PA]_0$ (M)	$\Delta S°$ (J/Kmol)	$\Delta H°$ (kJ/mol)	$\Delta G°$ (kJ/mol)				
			298 K	303 K	308 K	318 K	328 K
0.00	0.073	25.64	3.886	3.521	3.156	2.426	1.696
0.01	0.076	21.41	−1.238	−1.618	−1.998	−2.758	−3.518
0.05	0.183	52.03	−2.504	−3.419	−4.334	−6.164	−7.994
0.10	0.262	75.60	−2.476	−3.786	−5.096	−7.716	−10.34

an increase in the randomness after sorption and the sorption is entropy driven.

4. Conclusions

The present study reveals that the addition of PA to limestone powder considerably increases the removal of fluoride. The experimental observations suggest that the selective removal of fluoride by PA-enhanced limestone is mainly governed by both physical adsorption and ion exchange. The *in situ* formed calcium phosphate or HAP is responsible for the increased fluoride removal. The limestone surface acts only as a minor adsorbent. Analysis of the solid after sorption experiment also showed sorption of fluoride on limestone surface along with the presence of HAP and FAP.

The defluoridation with limestone increases with increase in $[PA]_0$ concentrations. The kinetics of sorption of fluoride fits the different kinetic models in the following order: pseudo-second-order > pseudo-first-order > Elovich > intraparticle diffusion. The fluoride adsorption fits to different adsorption models in the order: Temkin > Freundlich > D–R > Langmuir. The maximum adsorption capacity has been estimated to be 4.38 mg/g which is comparable with HAP and brushite. The PA-enhanced limestone is advantageous also over other high capacity-modified adsorbents as it does not involve any sophisticated or energy-intensive technology and therefore, has a great potential for applications in fluoride removal in countries where HAP and brushite do not occur naturally. The thermodynamic calculations showed that the adsorption and/or ion exchange of fluoride on PA-enhanced limestone was spontaneous and endothermic in nature.

References

[1] A.K. Susheela, A Treatise on Fluorosis, Fluorosis Research and Rural Development Foundation, New Delhi, 2001.
[2] M. Mohapatra, S. Anand, B.K. Mishra, D.E. Giles, P. Singh, Review of fluoride removal from drinking water, J. Environ. Manage. 91 (2009) 67–77.
[3] A. Bhatnagar, E. Kumar, M. Sillanpaa, Fluoride removal from water by adsorption—A review, Chem. Eng. J. 171 (2011) 811–840.
[4] S.K. Nath, R.K. Dutta, Significance of calcium containing materials for defluoridation of water: A review, Desalin. Water Treat. (in press) doi: 10.1080/19443994.2013.866056.
[5] R.K. Dutta, G. Saikia, B. Das, C. Bezbaruah, H.B. Das, S.N. Dube, Fluoride contamination in groundwater of central Assam, India, Asian J. Water Environ. Pollut. 2 (2006) 93–100.
[6] B. Das, J. Talukdar, S. Sarma, B. Gohain, R.K. Dutta, H.B. Das, S.C. Das, Fluoride and other inorganic constituents in groundwater of Guwahati, Assam, India, Curr. Sci. 85 (2003) 657–661.
[7] World Health Organization (WHO), Guideline for Drinking-water Quality, fourth ed., IWA (International Water Association), Geneva, 2011, pp. 370–371.
[8] Bureau of Indian Standards (BIS), Indian Standard Specification for Drinking Water, IS 10500, Bureau of Indian Standards, New Delhi, 1991, pp. 2–4.
[9] A.K.M. Fazlul Hoque, M. Khaliquzzaman, M.D. Hossain, A.H. Khan, Fluoride levels in different drinking water sources in Bangladesh, Fluoride 36 (2003) 38–44.
[10] E.W. Wambu, C.O. Onindo, W. Ambusso, G.K. Muthakia, Removal of fluoride from aqeuous solution by adsorption using a siliceous mineral of a Kenyan Origin, Clean — Soil, Air, Water 41 (2013) 340–348.
[11] E. Abdessalem, B. Ahmed, H. Ahmed, B. Nasr, Removal of fluoride from aluminum fluoride manufacturing wastewater by precipitation and adsorption processes, Desalin. Water Treat. (in press) doi: 10.1080/19443994.2014.899515.
[12] A. Ben Nasr, K. Walha, C. Charcosset, R. Ben Amar, Removal of fluoride ions using cuttlefish bones, J. Fluorine Chem. 132 (2011) 57–62.
[13] S. Basudevan, J. Lakshmi, G. Sozhan, Studies on a Mg-Al-Zn alloy as an anode for the removal of fluoride from drinking water in an electrocoagulation process, Clean — Soil, Air, Water 37 (2009) 370–378.

[14] M. Arda, E. Orhan, O. Arar, M. Yuksel, N. Kabay, Removal of fluoride from geothermal water by electrodialysis (ED), Sep. Sci. Technol. 44 (2009) 841–853.

[15] M. Mohapatra, K. Rout, P. Singh, S. Anand, S. Layek, H.C. Verma, B.K. Mishra, Fluoride adsorption studies on mixed–phase nano iron oxides prepared by surfactant mediation-precipitation technique, J. Hazard. Mater. 186 (2011) 1751–1757.

[16] T. Matsuura, S. Sourirajan, Studies on reverse osmosis for water pollution control, Water Res. 6 (1972) 1073–1086.

[17] P. Sehn, Fluoride removal with extra low energy reverse osmosis membranes: Three years of large scale field experience in Finland, Desalination 223 (2008) 73–84.

[18] M. Tahaikt, R. El Habbani, A. Ait Haddou, I. Achary, Z. Amor, M. Taky, A. Alami, A. Boughriba, M. Hafsi, A. Elmidaoui, Fluoride removal from groundwater by nanofiltration, Desalination 212 (2007) 46–53.

[19] A. Ben Nasr, C. Charcosset, R. Ben Amar, K. Walha, Defluoridation of water by nanofiltration, J. Fluorine Chem. 150 (2013) 92–97.

[20] X. Fan, D.J. Parker, M.D. Smith, Adsorption kinetics of fluoride on low cost materials, Water Res. 37 (2003) 4929–4937.

[21] Y. Cengeloglu, E. Kir, M. Ersoz, Removal of fluoride from aqueous solution by using red mud, Sep. Purif. Technol. 28 (2002) 81–86.

[22] A. Tor, N. Danaoglu, G. Arslan, Y. Cengeloglu, Removal of fluoride from water by using granular red mud: Batch and column studies, J. Hazard. Mater. 164 (2009) 271–278.

[23] B. Thole, F. Mtalo, W. Masamba, Groundwater defluoridation with raw bauxite, gypsum, magnesite, and their composites, Clean — Soil, Air, Water 40 (2012) 1222–1228.

[24] C. Kayira, S. Sajidu, W. Masamba, J. Mwatseteza, Defluoridation of groundwater using raw bauxite: Kinetics and thermodynamics, Clean — Soil, Air, Water 42 (2014) 546–551, doi: 10.1002/clen.201200488.

[25] A. Maiti, J.K. Basu, S. De, Chemical treated laterite as fluoride adsorbent for aqueous system and kinetic modelling, Desalination 265 (2011) 28–36.

[26] M. Sarkar, A. Banerjee, P.P. Pramanik, A.R. Sarkar, Use of laterite for the removal of fluoride from contaminated drinking water, J. Colloid Interface Sci. 302 (2006) 432–444.

[27] M. Agarwal, K. Rai, R. Shrivastav, S. Dass, Deflouridation of water using amended clay, J. Clean Prod. 11 (2003) 439–444.

[28] A.D. Atasoy, M.O. Sahin, Adsorption of fluoride on the raw and modified cement clay, Clean — Soil, Air, Water 41 (2013) 1–6, doi: 10.1002/clen.201300074.

[29] M. Mourabet, H. El Boujaady, A. El Rhilassi, H. Ramdane, M. Bennani-Ziatni, R. El Hamri, A. Taitai, Defluoridation of water using Brushite: Equilibrium, kinetic and thermodynamic studies, Desalination 278 (2011) 1–9.

[30] A.M. Raichur, M.J. Basu, Adsorption of fluoride onto mixed rare earth oxides, Sep. Purif. Technol. 24 (2001) 121–127.

[31] H. Lounici, L. Addour, D. Belhocine, H. Grib, S. Nicolas, B. Bariou, N. Mameri, Study of a new technique for fluoride removal from water, Desalination 114 (1997) 241–251.

[32] G.E.J. Poinern, M.K. Ghosh, Y.J. Ng, T.B. Issa, S. Anand, P. Singh, Defluoridation behavior of nano-structured hydroxyapatite synthesized through an ultrasonic and microwave combined technique, J. Hazard. Mater. 185 (2011) 29–37.

[33] Y.H. Li, S. Wang, A. Cao, D. Zhao, X. Zhang, C. Xu, Z. Luan, D. Ruan, J. Liang, D. Wu, B. Wei, Adsorption of fluoride from water by amorphous alumina supported on carbon nanotubes, Chem. Phys. Lett. 350 (2001) 412–416.

[34] C.S. Sundaram, N. Viswanathan, S. Meenakshi, Fluoride sorption by nanohydroxyapatite/chitin composite, J. Hazard. Mater. 172 (2009) 147–151.

[35] D.L. Mawaniki, J.M. Simwa, F. Manji, Fluoride binding capacity of bone charcoal and its effects on selected micro-organisms, East Afr. Med. J. 67 (1990) 427–431.

[36] G. Asgari, B. Roshani, G. Ghanizadeh, The investigation of kinetic and isotherm of fluoride adsorption onto functionalize pumice stone, J. Hazard. Mater. 217–218 (2012) 123–132.

[37] Y. Li, P. Zhang, Q. Du, X. Peng, T. Liu, Z. Wang, Y. Xia, W. Zhang, K. Wang, H. Zhu, D. Wu, Adsorption of fluoride from aqueous solution by graphene, J. Colloid Interface Sci. 363 (2011) 348–354.

[38] V. Sivasankara, S. Rajkumara, S. Murugeshb, A. Darchen, Tamarind (Tamarindus indica) fruit shell carbon: A calcium-rich promising adsorbent for fluoride removal from groundwater, J. Hazard. Mater. 225–226 (2012) 164–172.

[39] Y.H. Li, S. Wang, X. Zhang, J. Wei, C. Xu, Z. Luan, D. Wu, Adsorption of fluoride from water by aligned carbon nanotubes, Mater. Res. Bull. 38 (2003) 469–476.

[40] S.K. Nath, R.K. Dutta, Enhancement of limestone defluoridation of water by acetic and citric acids in fixed bed reactor, Clean — Soil, Air, Water 38 (2010) 614–622.

[41] S.K. Nath, R.K. Dutta, Acid-enhanced limestone defluoridation in column reactor using oxalic acid, Process Saf. Environ. Prot. 90 (2012) 65–75.

[42] A. Ben Nasr, K. Walha, F. Puel, D. Mangin, R. Ben Amar, C. Charcosset, Precipitation and adsorption during fluoride removal from water by calcite in the presence of acetic acid, Desalin. Water Treat. 52 (2014) 2231–2240.

[43] M. Jimenez-Reyes, M. Solache-Rios, Sorption behavior of fluoride ions from aqueous solutions by hydroxyapatite, J. Hazard. Mater. 180 (2010) 297–302.

[44] Y. Wang, N. Chen, W. Wei, J. Cui, Z. Wei, Enhanced adsorption of fluoride from aqueous solution onto nanosized hydroxyapatite by low-molecular-weight organic acids, Desalination 276 (2011) 161–168.

[45] S.K. Nath, R.K. Dutta, Fluoride removal from water using crushed limestone, Indian J. Chem. Technol. 17 (2009) 120–125.

[46] E. Kumar, A. Bhatnagar, U. Kumar, M. Sillanpaa, Defluoridation from aqueous solutions by nano-alumina: Characterization and sorption studies, J. Hazard. Mater. 186 (2011) 1042–1049.

[47] M. Islam, P.C. Mishra, R. Patel, Physicochemical characterization of hydroxyapatite and its application towards removal of nitrate from water, J. Environ. Manage. 91 (2010) 1883–1891.

[48] H. Tahir, Comparative trace metal contents in sediments and the removal of chromium using Zeolite-5A, EJEAFChe. 4 (2005) 1021–1032.

[49] B.D. Turner, P.J. Binning, S.W. Sloan, Impact of phosphate on fluoride removal by calcite, Environ. Eng. Sci. 27 (2010) 643–650.

[50] C. Murutu, M.S. Onyango, A. Ochieng F.AO. Otieno, Fluoride removal performance of phosphoric acid treated lime: Breakthrough analysis and point-of-use system performance, Water SA 38 (2012) 279–285.

[51] W.G. Nawlakhe, D.N. Kulkarni, B.N. Pathak, K.R. Bulusu, Defluoridation using the Nalgonda Technique in Tanzania, Ind. J. Environ. Health 17 (1975) 26–65.

[52] C.S. Sundaram, N. Viswanathan, S. Meenakshi, Defluoridation chemistry of synthetic hydroxyapatite at nano scale: Equilibrium and kinetic studies, J. Hazard. Mater. 155 (2008) 206–215.

[53] E. Beniash, R.A. Metzler, R.S.K. Lam, P.U.P.A. Gilbert, Transient amorphous calcium phosphate in forming enamel, J. Struct. Biol. 166 (2009) 133–143.

[54] M.M. Khunur, A. Risdianto, S. Mutrofin, Y.P. Prananto, Synthesis of fluorite (CaF_2) crystal from gypsum waste of phosphoric acid factory in silica gel, Bull. Chem. Eng. Catal. 7 (2012) 71–77.

[55] S.K. Nath, S. Bordoloi, R.K. Dutta, Effect of acid on morphology of calcite during acid enhanced defluoridation, J. Fluorine Chem. 132 (2011) 19–26.

[56] W. Augustyn, M. Dziegielewska, A. Kossuth, Z. Librant, Studies of the reaction of crystalline calcium carbonate with aqueous solutions of NH_4F, KF and NaF, J. Fluorine Chem. 12 (1978) 281–292.

[57] R. Aldaco, A. Garea, A. Irabien, Fluoride recovery in a fluidized bed: Crystallization of calcium fluoride on silica sand, Ind. Eng. Chem. Res. 45 (2006) 796–802.

[58] E.J. Reardon, Y. Wang, A limestone reactor for fluoride removal from wastewater, Environ. Sci. Technol. 34 (2000) 3247–3253.

[59] S. Kagne, S. Jagtap, P. Dhawade, S.P. Kamble, S. Devotta, S.S. Rayalu, Hydrated cement: A promising adsorbent for the removal of fluoride from aqueous solution, J. Hazard. Mater. 154 (2008) 88–95.

[60] S. Ming-Cheng, Kinetics of the batch adsorption of methylene blue from aqueous solutions onto rice husk: Effect of acid-modified process and dye concentration, Desalin. Water Treat. 37 (2012) 200–214.

[61] K. Kadirvelu, C. Faur-Brasquet, P. Le Cloiree, Removal of Cu(II), Pb(II), and Ni(II) by adsorption onto activated carbon cloths, Langmuir 16 (2000) 8404–8409.

[62] M. Islam, P.C. Mishra, R. Patel, Physicochemical characterization of hydroxyapatite and its application towards removal of nitrate from water, J. Environ. Manage. 91 (2010) 1883–1891.

[63] C. Aharoni, F.C. Tompkins, Kinetics of adsorption and desorption and the Elovich equation, in: D.D. Eley, H. Pines, P.B. Weisz (Eds.), Advance in Catalysis and Related Subjects, Academic press, New York, NY, 1970, pp. 1–49.

[64] R. Huang, B. Yang, Q. Liu, K. Ding, Removal of fluoride ions from aqueous solutions using protonated cross-linked chitosan particles, J. Fluorine Chem. 141 (2012) 29–34.

[65] K.R. Hall, L.C. Eagleton, A. Acrivos, T. Vermeulen, Pore- and solid-diffuion kinetics in fixed-bed adsorption under constant-pattern conditions, Ind. Eng. Chem. Fundam. 5 (1966) 212–223.

[66] W. Nigussie, F. Zewge, B.S. Chandravanshi, Removal of excess fluoride from water using waste residue from alum manufacturing process, J. Hazard. Mater. 147 (2007) 954–963.

[67] M.I. Temkin, V. Pyzhev, Kinetics of ammonia synthesis on promoted iron catalysts, Acta Physiochim. URSS 12 (1940) 327–356.

[68] G.E. Boyd, Q.V. Larson, S. Lindenbaum, Heat capacity changes in ion-exchange reactions. The exchange of tetra-n-butylammonium with sodium ion in cross-linked polystyrenesulfonatel, J. Phys. Chem. 72 (1968) 2651–2654.

[69] O. Ismail, O. Utkan, O. Bilge, V. Sevil, Kinetic, thermodynamic, and equilibrium studies for adsorption of azo reactive dye onto a novel waste adsorbent: Charcoal ash, Desalin. Water Treat. 52 (2013) 6091–6100.